The Abdus Salam
International Centre for Theoretical Physics

United Nations
Educational, Scientific and
Cultural Organization

IAEA
International Atomic Energy Agency

2137-40

Joint ICTP-IAEA Advanced Workshop on Multi-Scale Modelling for Characterization and Basic Understanding of Radiation Damage Mechanisms in Materials

12 - 23 April 2010

Experimental simulation of nuclear fuels: separate effect studies (Part 4)

M. Freyss
CEA, Centre de Cadarache
Saint Paul lez Durance
France

Part 4

Experimental simulation of nuclear fuels: separate effect experiments

Objectives of the separate effect studies

- **To model and to understand nuclear fuel behavior under irradiation** as well as under long term storage conditions
  - Volatile fission products I, Xe, Kr, Cs + He
  - Transport properties
  - Irradiation effects

- **Direct support to modeling**
  - Guide: mechanism understanding
  - Basic data to be used in the models

- **Experimental and theoretical methodologies developed for application to a large panel of materials**
  - Oxides UO_2 and MOX $(U,Pu)O_2$
  - Carbides UC and UPuC…

Separated effects studies : the approach

- Non active model materials such as UO_2
- Ion **implantation** to simulate FP
- **Thermal treatment or** heavy ion **irradiation**

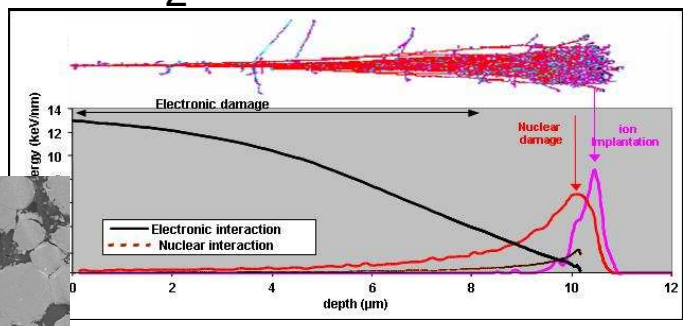

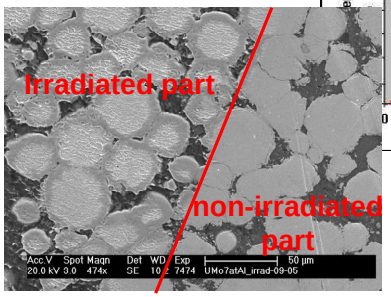

- **Characterization with a large panel of dedicated techniques** (SIMS, RBS, NRA, TEM, XAS…)

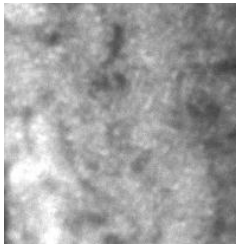

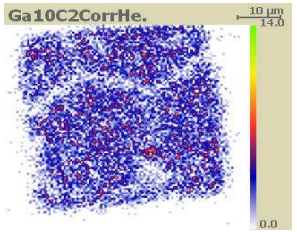

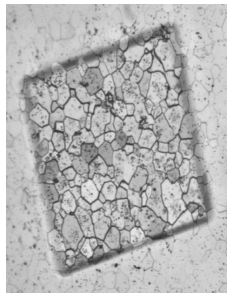

- **Large scientific facilities** (particle accelerators and synchrotron radiation)

Separated effects studies : illustrations

	Objective	Studies
1	Understand and model fission gas diffusion/ precipitation/release in nuclear oxide fuels	XAS and TEM characterization of Xe bubbles in uranium dioxide
2	Understand and model He behavior in nuclear oxide fuels	Thermal diffusion of helium in uranium dioxide
3	Oxygen diffusion in relation to p-type doping in UO_2	Electrical conductivity and diffusion coefficient measurements in UO_2

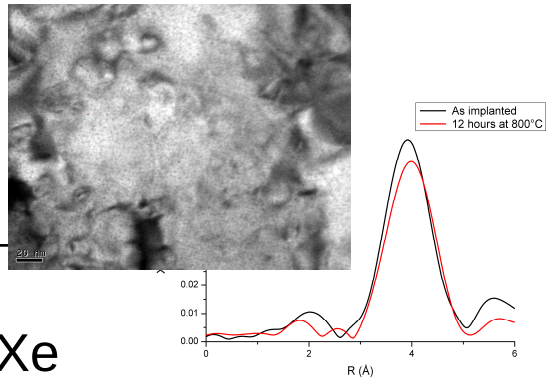

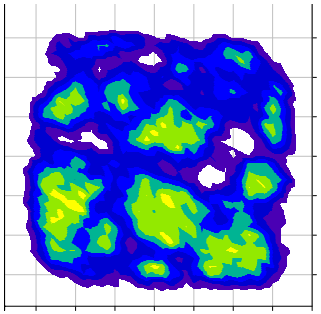

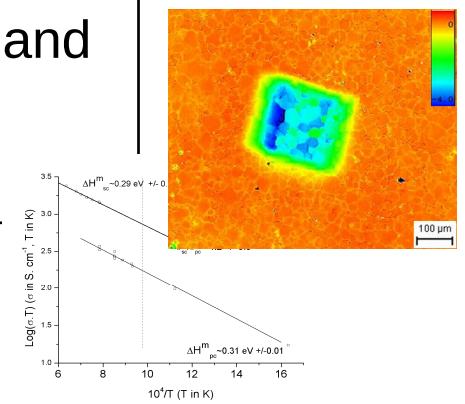

Separated effects studies : illustrations

	Objective	Studies
1	Understand and model fission gas diffusion/ precipitation/release in nuclear oxide fuels	XAS and TEM characterization of Xe bubbles in uranium dioxide
2	Understand and model He behavior in nuclear oxide fuels	Thermal diffusion of helium in uranium dioxide
3	Oxygen diffusion in relation to p-type doping in UO_2	Electrical conductivity and diffusion coefficient measurements in UO_2

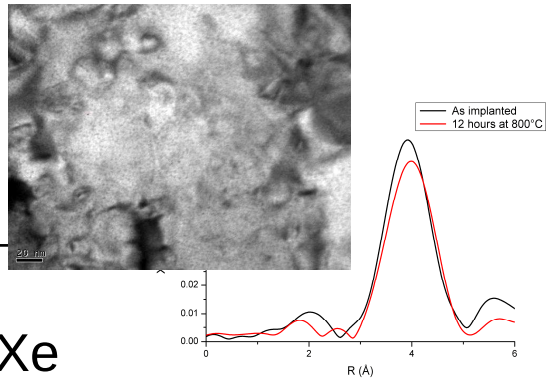

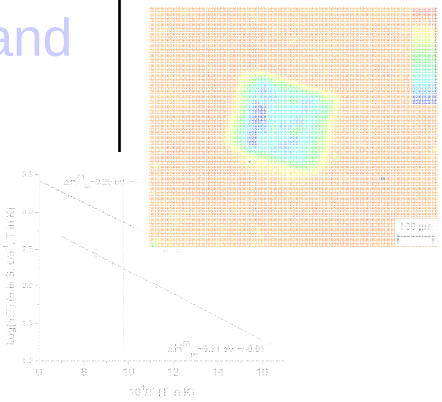

XAS and TEM characterization of Xe bubbles in UO_2

Issue : Understand and model xenon release in nuclear oxide fuels

- Rare gases are highly **insoluble** in most materials
  (confirmed by 1st-principles and empirical potential calculations)

- Therefore predicting rare gas **transport** requires:
  * understanding precipitation mechanisms
  * rare gas bubble characteristics
  * diffusion of gas atoms in presence of bubbles

- Two analytical tools are very powerful when coupled :

Transmission electron microscopy (**TEM**) and X-ray absorption spectroscopy (**XAS**)

XAS and TEM characterization of Xe bubbles in UO_2

Understanding of thermally activated phenomena : post-irradiation annealing on irradiated fuel

- High temperature (>~1300℃) anneals of irradiated material
- At a given temperature, three stages generally identified (*Valin, Portier, PhD theses 1999-2005)*
  - (1) instantaneous release: gas accumulated at grain boundaries
  - (2) diffusion controlled release
  - (3) fractional release levels off

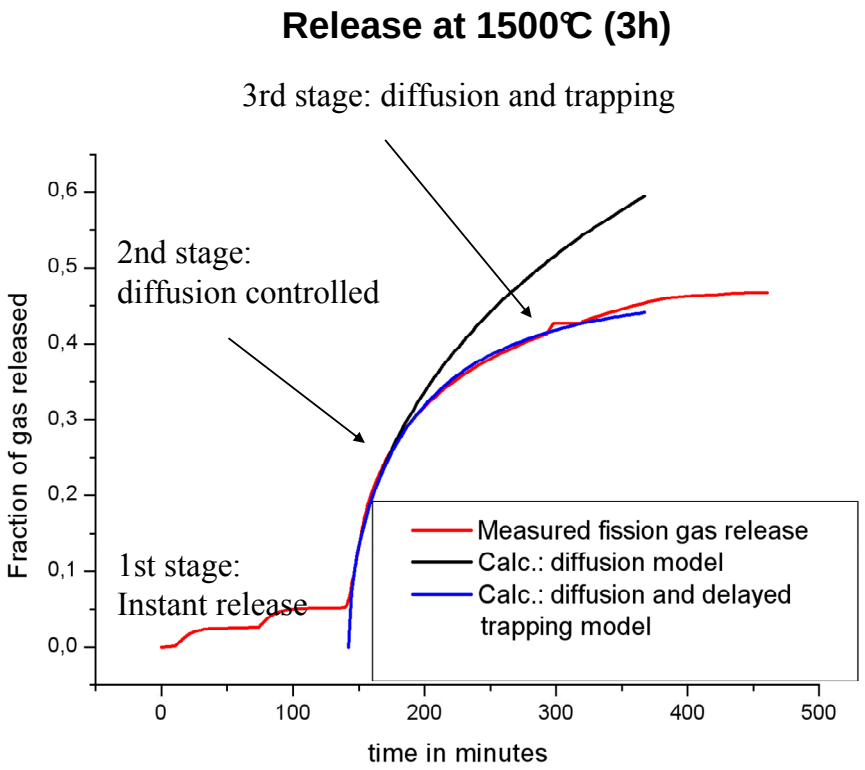

Trapping efficiency?
Characteristic of bubbles?

XAS and TEM characterization of Xe bubbles in UO_2

What information can we get from in situ transmission electron microscopy (TEM)?

- Defect accumulation/annealing
- Threshold temperature for bubble precipitation
- Bubble size distribution
- Electronic excitation effects: bubble nucleation and fission gas re-solution

TEM measurements by C. Sabathier *et al.* (CEA/DEC Cadarache)

Methodology

- *In situ* TEM experiments carried out in Orsay: IRMA (now JANNUS beam line)
- 390 keV Xe implanted UO_2 thin foils (Rp~60nm)
- Samples are observed at increasing doses and annealed for approx. 20 min. at various temperatures

XAS and TEM characterization of Xe bubbles in UO_2

Xe bubble precipitation: main results of TEM study

[Xe]	2.10^{15} Xe/cm² (0.4 at.%)	1.10^{16} Xe/cm² (2 at.%)
$T_{thresh.}$	600°C	400°C
Size (nm)	~ 1	2

$$T_{thres.} = f(C_{Xe})$$

⇨ defect concentrations

Annealing conditions	400°C ~ 20 min	600°C ~ 20 min
Bubble density (b/m³)	$3.0 .10^{23}$ $\pm 1.0.10^{23}$	**$4.0 .10^{23}$ $\pm 1.0.10^{23}$**
Bubble size (nm)	1.7 ± 0.3nm	1.8 ± 0.3nm

C. Sabathier *et al.* NIMB 266, 3027 (2008)

TEM observations on 2 at.% sample annealed at 600℃ for 20 minutes

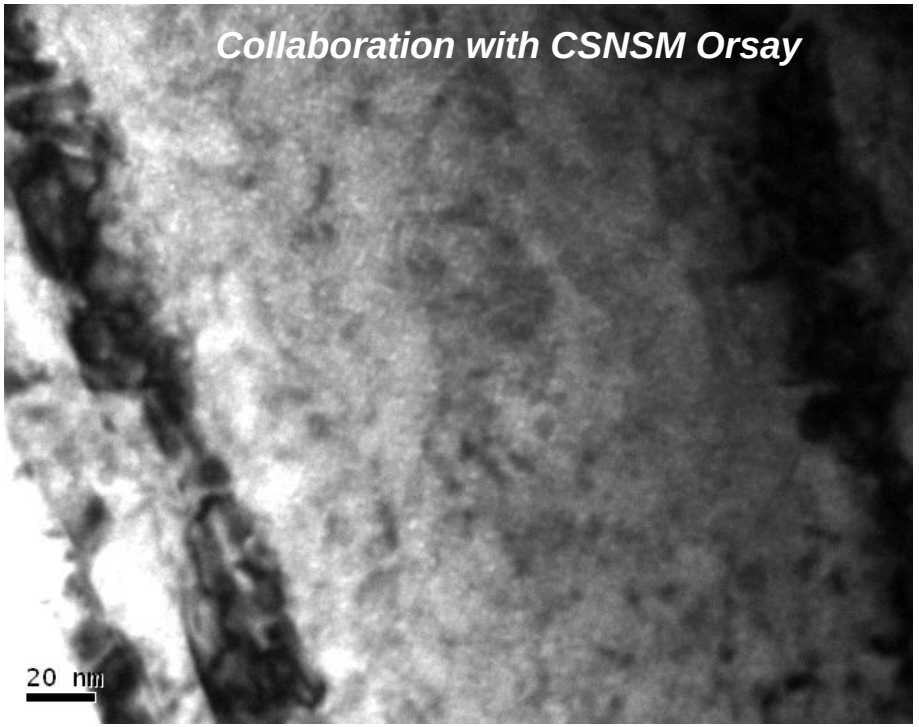

Same results obtained on irradiated UO_2 fuel, 49 GWd/Mt (0.5 at%), T~600℃ :

$4.3\ 10^{23}$ b/m³ [Nogita *et al. NIMB 141, 481 (1998)*]

XAS and TEM characterization of Xe bubbles in UO_2

What information can we get from X-ray absorption spectroscopy (XAS)?

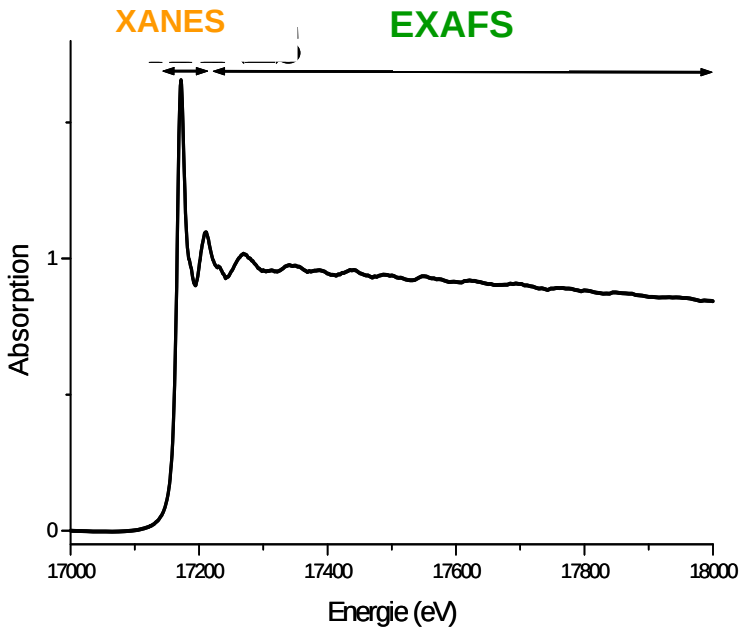

Determination of element local environment

EXAFS & XANES

Extended X-ray Absorption Fine Structure

- **Inter-atomic distances**
- **Number of nearest neighbours**
- **Thermal agitation**

Complete description of local environment

X-ray Absorption Near Edge Structure

- **Oxidation state**
- **Local symmetry**

1° RG-RG distance

XAS and TEM characterization of Xe bubbles in UO_2

XAS sample preparation

- Polycrystalline UO_2 pellets
- **Ion Xe implantation** Influence of concentration on bubble precipitation
  - Multi-energy ion implantation 2 at.% ($E \leq 800$ keV)
  - Single-energy implantation ~8 at.% max ($E=800$ keV, 10^{17} $Xe.cm^{-3}$, depth ~140 nm from surface)
- **Annealing** for precipitation/stability study of xenon bubbles
  - Annealing between 600℃ and 800℃ under reducing atmosphere

XAS and TEM characterization of UO_2

XAS experiment performed and data interpretation methodology

- Probe at the atomic scale, work performed mainly at low T(4-11K)
- Experiments performed on ESRF/FAME (BM30B), at Xe (34,5 keV) & Kr (14,3 keV) **K-edges**

Information relative to rare gas aggregates

$d_{Rg\text{-}Rg}$ → **lattice parameter** → **molar volume** —E.O.S.→ **aggregate internal pressure**

Number of neighbors —Geometrical considerations→ **indication of bubble size**

XAS and TEM characterization of Xe bubbles in UO_2

XAS bubble characterization: concentration effect

- **As implanted samples**
  - 2 at. % sample : no Xe-Xe bonds, no bubble nucleation / same conclusion using TEM
  - 8 at. % sample : bubble nucleation occurs

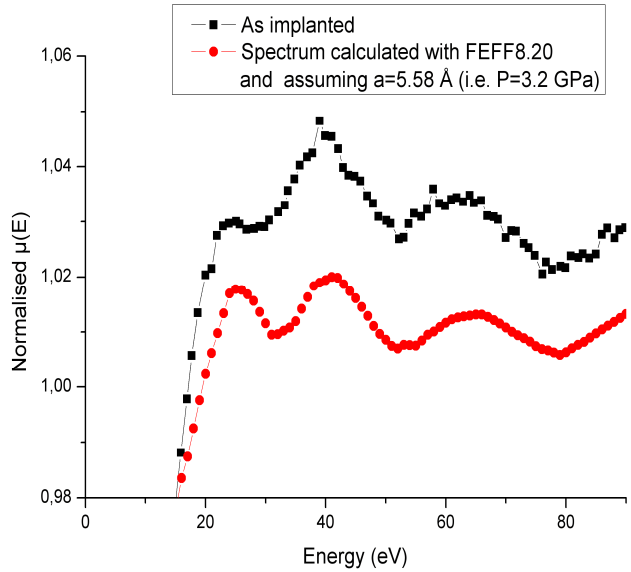

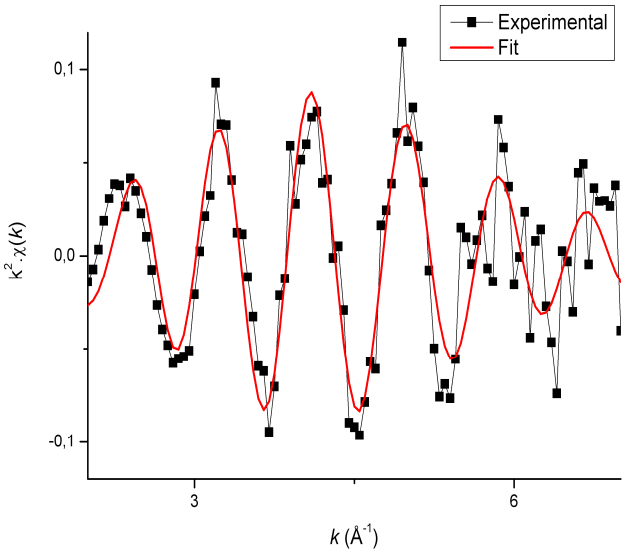

Only one Coordination shell

Xe-Xe distance estimated at 3.97 ± 0,02 Å against 4.39 Å for un-pressurised crystal

Then using an E.O.S., P=f(V,T) (K. Asaumi, Phys Rev. B 29(1984))

P ~ 2.8 ± 0.3 GPa

Bubble size ~ 1-2 nm

P. Garcia *et al*., J. Nucl. Mater. **352**, 136 (2006)

P. Martin *et al* Nucl. Instrum. and Meth. B **266**, 2887 (2008)

XAS and TEM characterization of Xe bubbles in UO_2

XAS bubble characterization: temperature effect

- **After annealing**
  - 2 at .% Xe sample / annealing **600℃** during 30 minutes

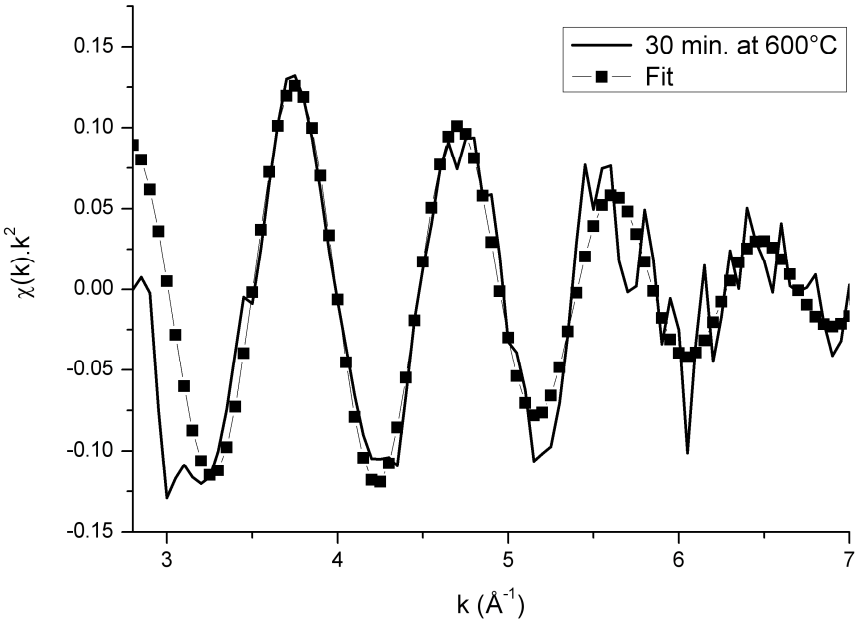

Xe-Xe bonds

bubble nucleation occurs

P. Garcia *et al*., J. Nucl. Mater. **352**, 136 (2006)
P. Martin *et al* Nucl. Instrum. and Meth. B **266**, 2887 (2008)

Same Xe local environment observed for the 8 at.% sample and for the as-implanted sample

P~ 2.8 ± 0.3 GPa,
Bubble size ~ 1-2 nm

XAS and TEM characterization of Xe bubbles in UO_2

XAS bubble characterization: temperature effect

- **After annealing**
  - 8 at .% Xe sample / annealing 12 hours at **600℃** and **800℃**

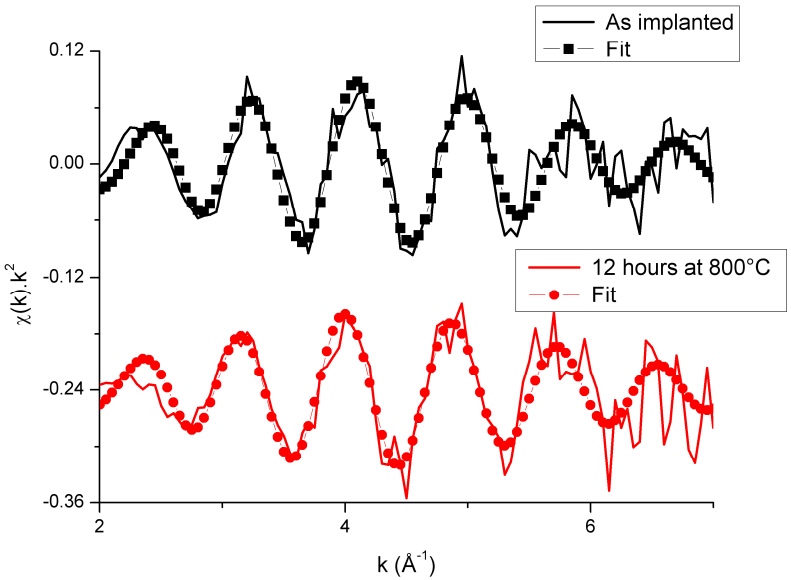

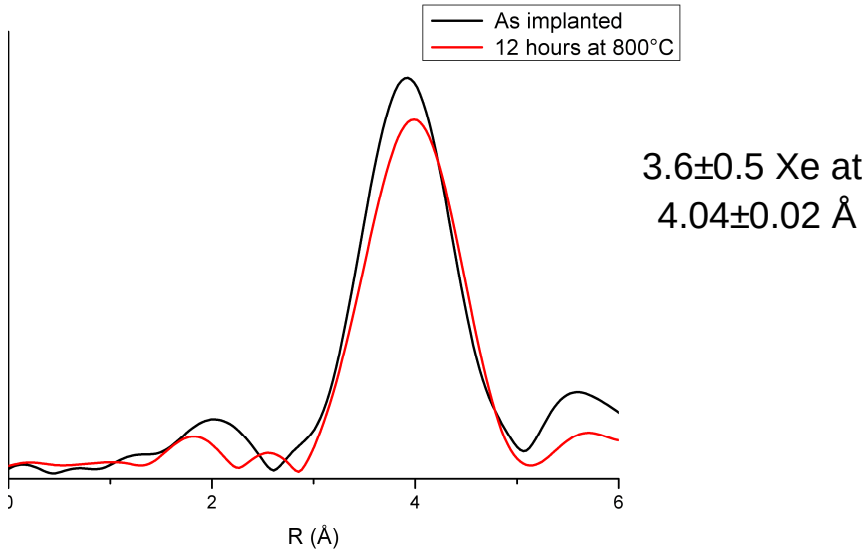

3.6±0.5 Xe at
4.04±0.02 Å

Small increase of Xe-Xe distance : Decrease of aggregate internal pressure **P~ 2.0 ± 0.3 GPa,**

No variation of N : Xenon bubbles remain small **Bubble size ~ 1-2 nm**

With annealing temperature up to 800℃:
Xenon aggregates remain small and highly pressurized (P~2.0 GPa)

P. Garcia *et al*., J. Nucl. Mater. **352**, 136 (2006) P. Martin *et al* NIMB. B **266**, 2887 (2008)

XAS and TEM characterization of Xe bubbles in UO_2

Coupling XAS and TEM : very useful to characterize rare gas bubbles

- XAS and TEM are efficient tools for characterising nanometer size bubble distributions
- Temperature induces xenon nucleation. So does irradiation by heavy ions (790 Mev Kr) in an inelastic or elastic energy loss regime (not presented): heterogeneous nucleation.
- Heavy ion (790 Mev Kr) irradiation induced xenon re-solution was not observed.
- Pressures within nanometer size rare gas aggregates are extremely high
- Provide very important data to be used in the modeling of nuclear fuel behaviour in pile

Separated effects studies : illustrations

	Objective	Studies
1	Understand and model fission gas diffusion/ precipitation/release in nuclear oxide fuels	XAS and TEM characterization of Xe bubbles in uranium dioxide
2	Understand and model He behavior in nuclear oxide fuels	Thermal diffusion of helium in uranium dioxide
3	Oxygen diffusion in relation to p-type doping in UO_2	Electrical conductivity and diffusion coefficient measurements in UO_2

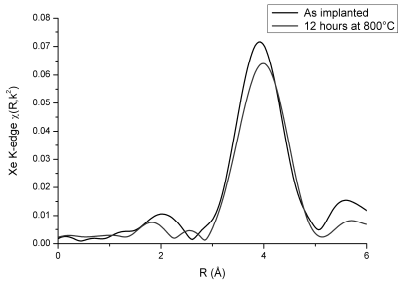

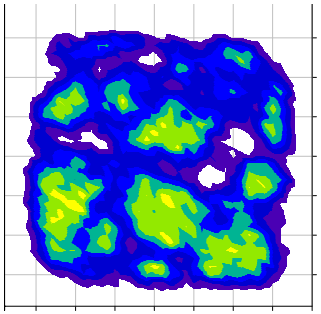

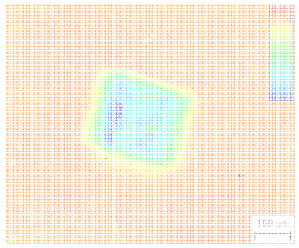

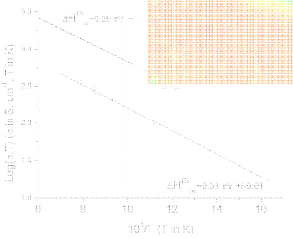

Thermo-diffusion of helium in uranium dioxide

Issue : Understand and model helium behavior in nuclear oxide fuels

- α-decay in spent fuels and minor actinides in fuel $\Rightarrow$ Helium accumulation

- Nuclear reaction analysis (**NRA**) methods using the **^{3}He(d,α)p reaction** to characterize helium behavior in fuel

Studies conducted by Guillaume Martin *et al.*
(CEA-Cadarache with CEMHTI Orléans – France)

Thermal diffusion of helium in uranium dioxide

Methodology and what we can get from NRA experiments

- 1. Helium implantation ^{3}He
- 2. Thermal annealing : helium migration, release
- 3. Analysis of helium remaining in the sample

NRA principle $^{3}He(^{2}H,^{4}He)^{1}H$

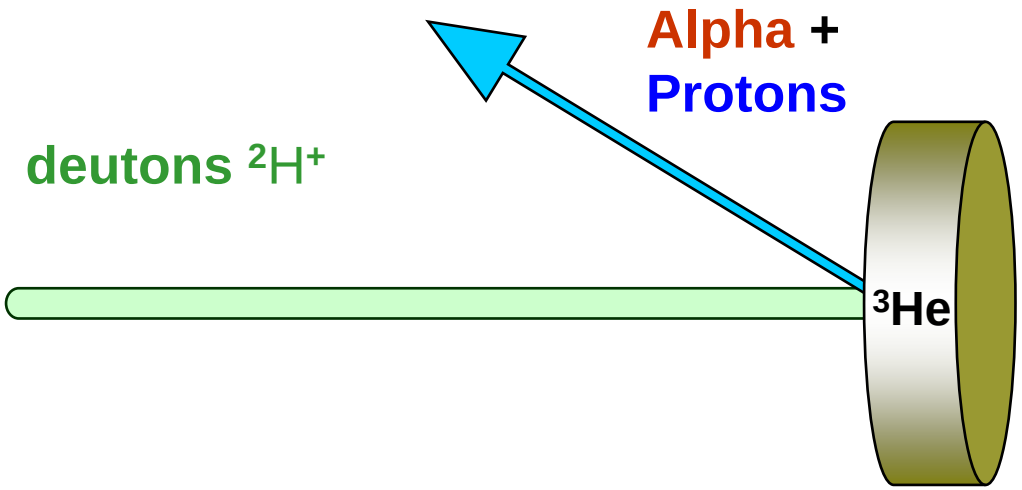

⇒ **3 techniques of characterization**

Thermal diffusion of helium in uranium dioxide

Three techniques for a 3-D characterization of He behavior: space x,y,z, time t, temperature T

<1> Desorption : t,T

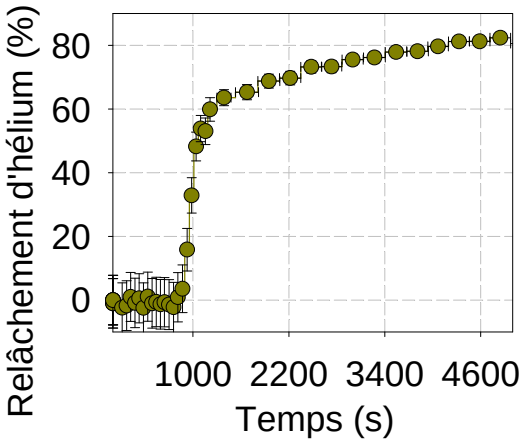

<2> Depth profiles 1D : z

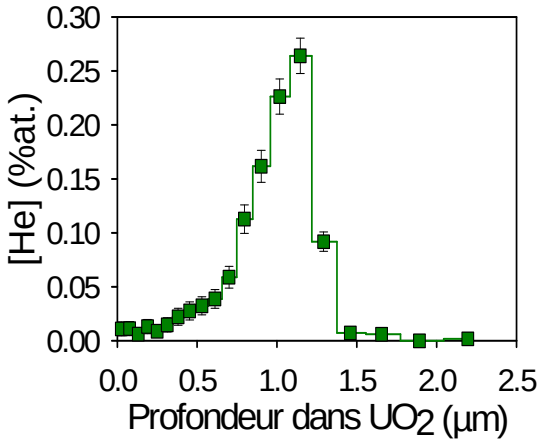

<3> 2D Cartography: x,y

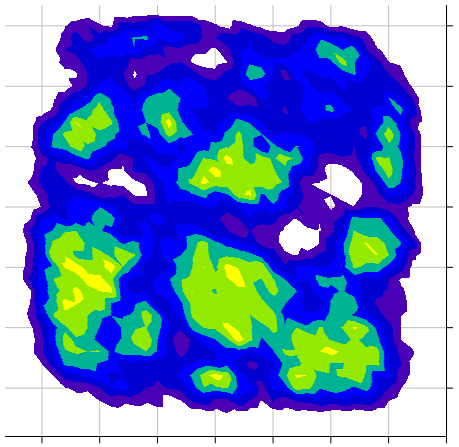

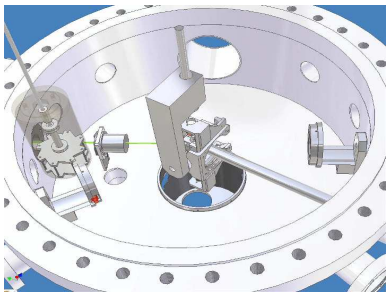

DIADDHEM (CEMHTI) : annealing and NRA measurements

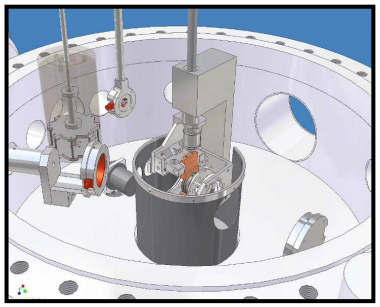

DIADDHEM : coincidence method

Labs involved:

- CNRS / CEMHTI (Orléans)
- CEA-CNRS / LPS (Saclay)

Thermal diffusion of helium in uranium dioxide

1-NRA: helium depth profiling

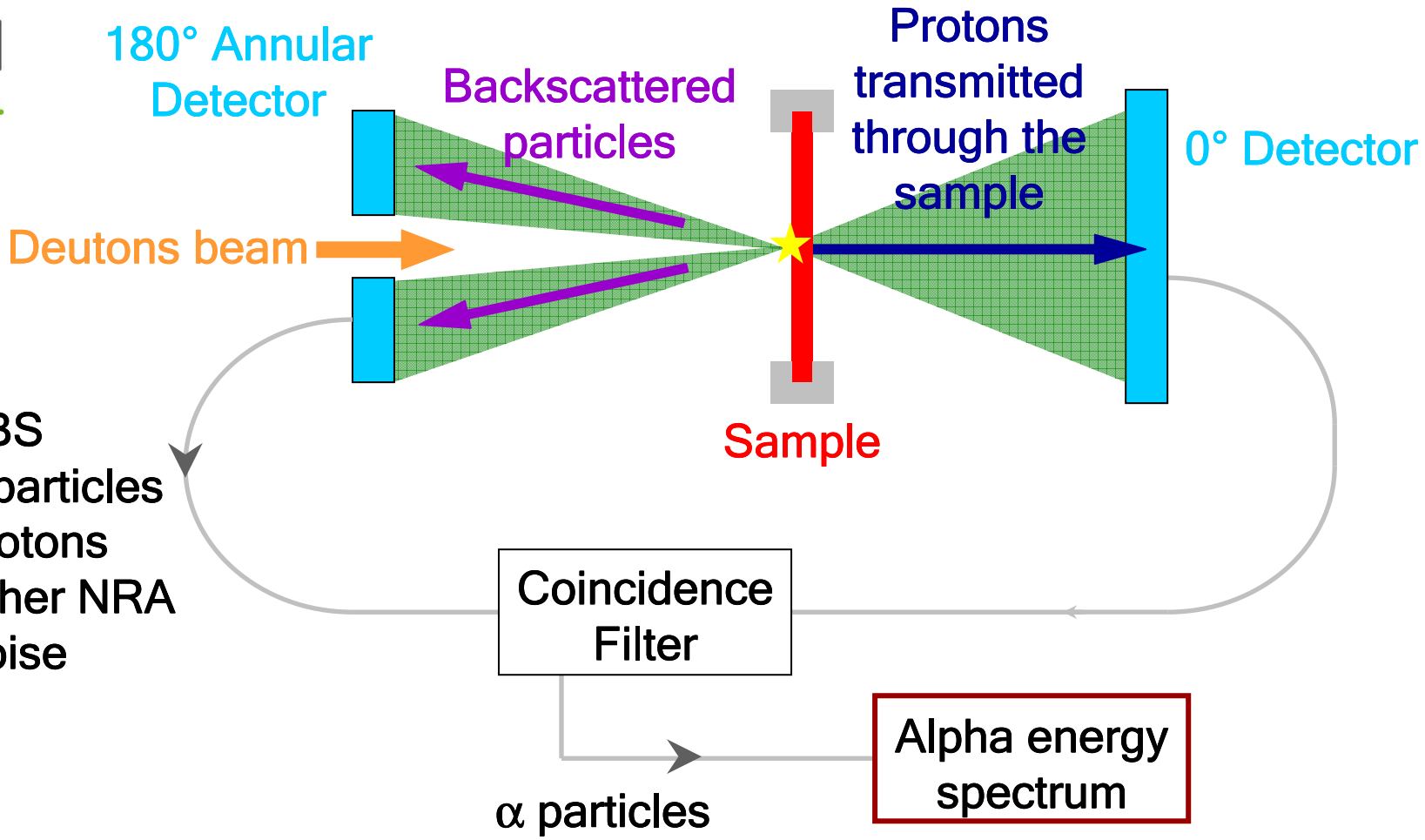

The greater the depth at which the α particle is produced within the sample, the more energy it loses as it reaches the sample surface

Thermal diffusion of helium in uranium dioxide

1-NRA: helium depth profiling, temperature effect

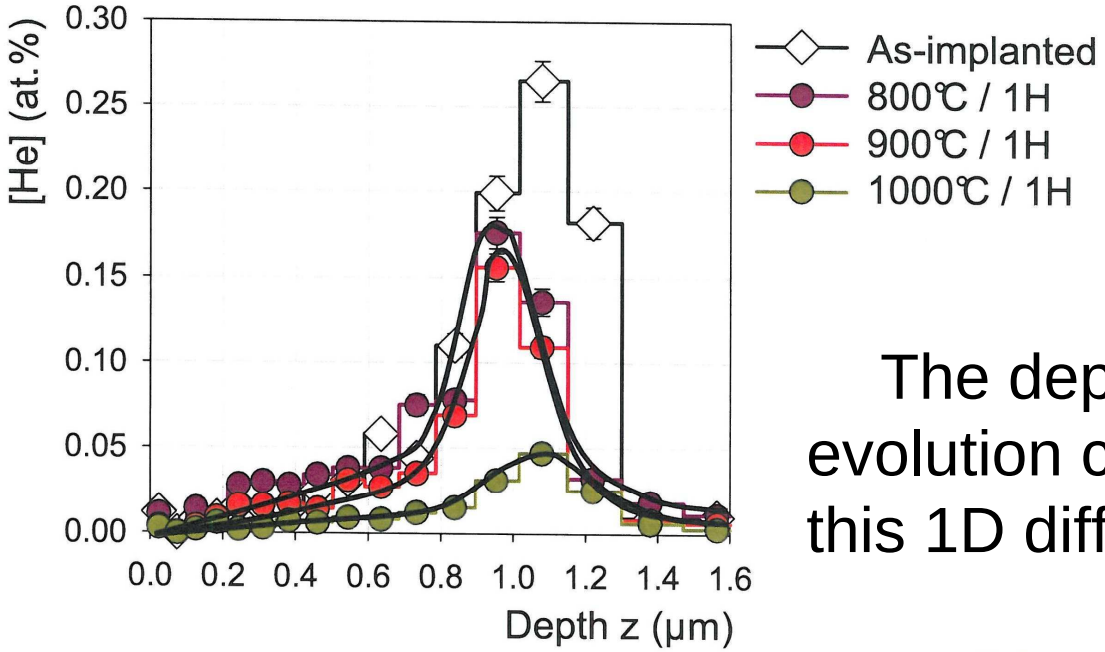

G.Martin *et al.*,
J. Nucl. Mater. 357, 198 (2006)

The depth profiles evolution can be modeled with this 1D diffusion equation:

Fick law *direct loss term* *drift term*

$$\frac{\partial C}{\partial t} = \frac{\partial}{\partial x}\left(D \frac{\partial}{\partial x} C \right) - kC - v\frac{\partial C}{\partial x}$$

Depth profiles after annealing do not broaden significantly: helium is able to migrate and is then **released via diffusion short-cuts such as grain boundaries**

Thermal diffusion of helium in uranium dioxide

2-NRA: helium release measurements

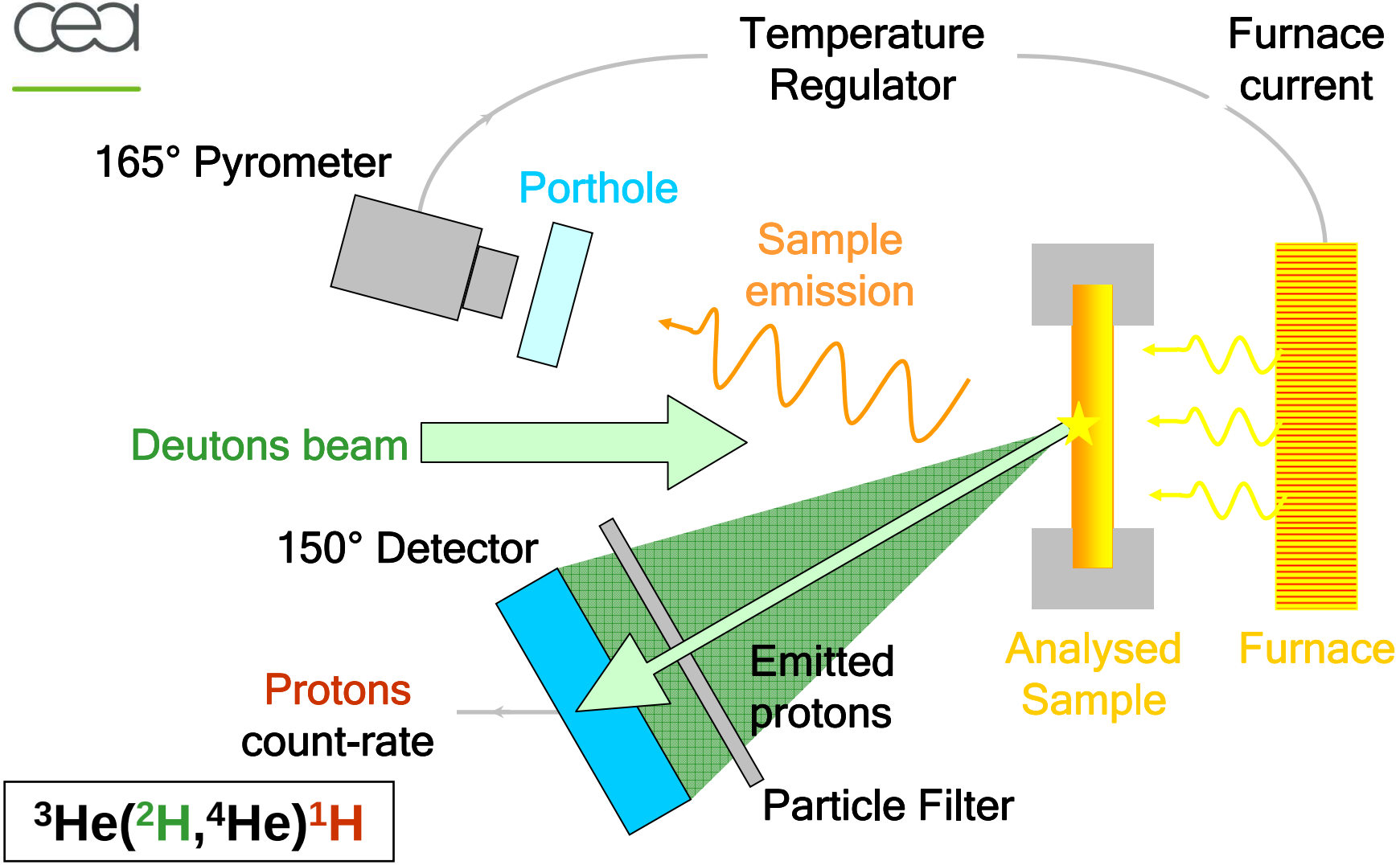

Thermal diffusion of helium in uranium dioxide

2-NRA helium release measurements :
Temperature effect on helium release

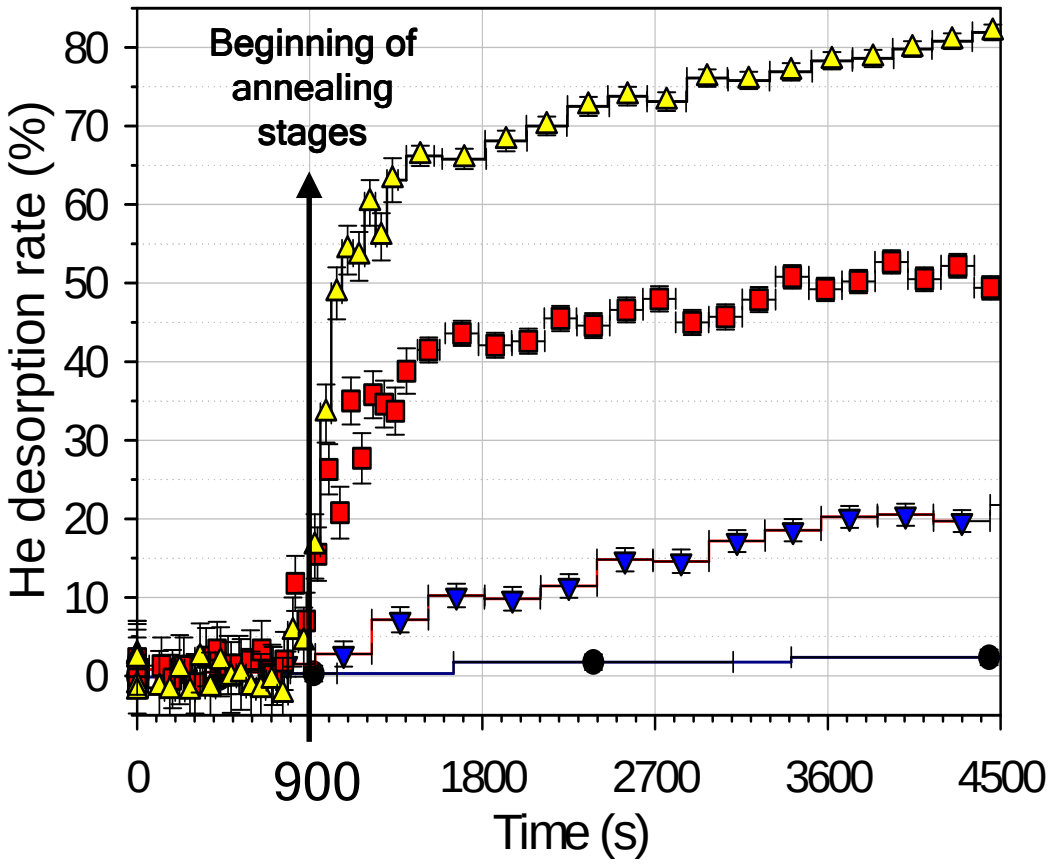

▲ : 1000°C/1H release 80%

■ : 900°C/1H release 50%

▼ : 800°C/1H release 20%

● : 700°C/4H release ~0%

At 800° C, helium release regular and slow.

Above 800° C, two successive stages. Fast transient helium release stage.

Thermal diffusion of helium in uranium dioxide

3- Micro-NRA: helium cartography

Measurement of remaining helium :

- Micrometric beam
- Analyzed area characterized by optic microscopy

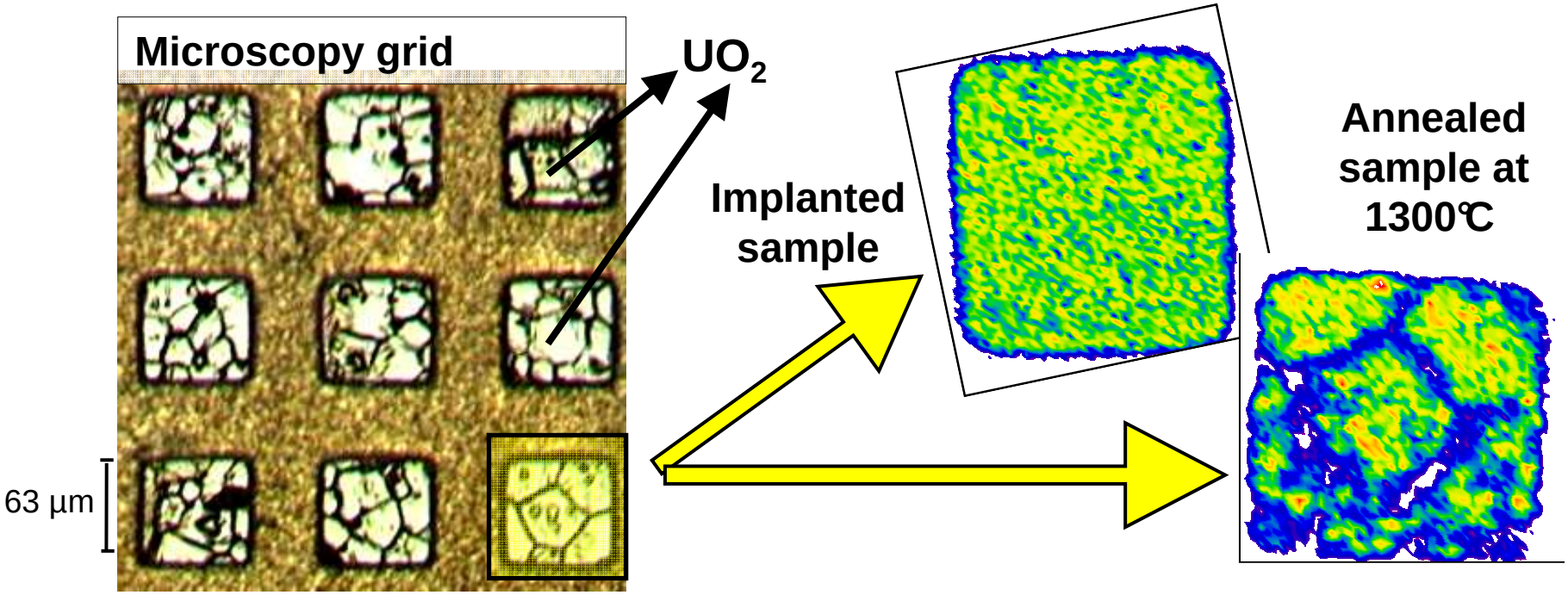

T. Sauvage *et al.*, NIMB **240**, 271 (2005)

µ-NRA consists in counting protons on every pixel scanned on the surface sample

Thermal diffusion of helium in uranium dioxide

μ–NRA helium cartography : microstructure effect

Scanning Electron Microscope image 63 μm

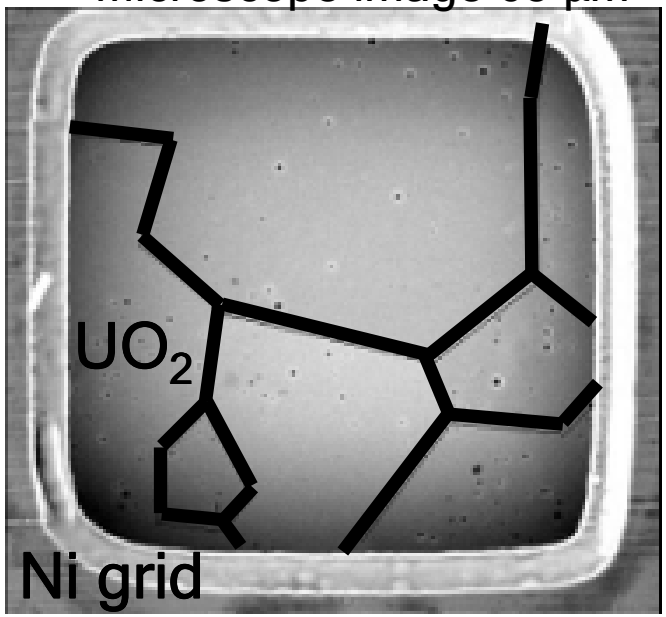

Helium relative content (%)

μ-NRA cartography 1000°C

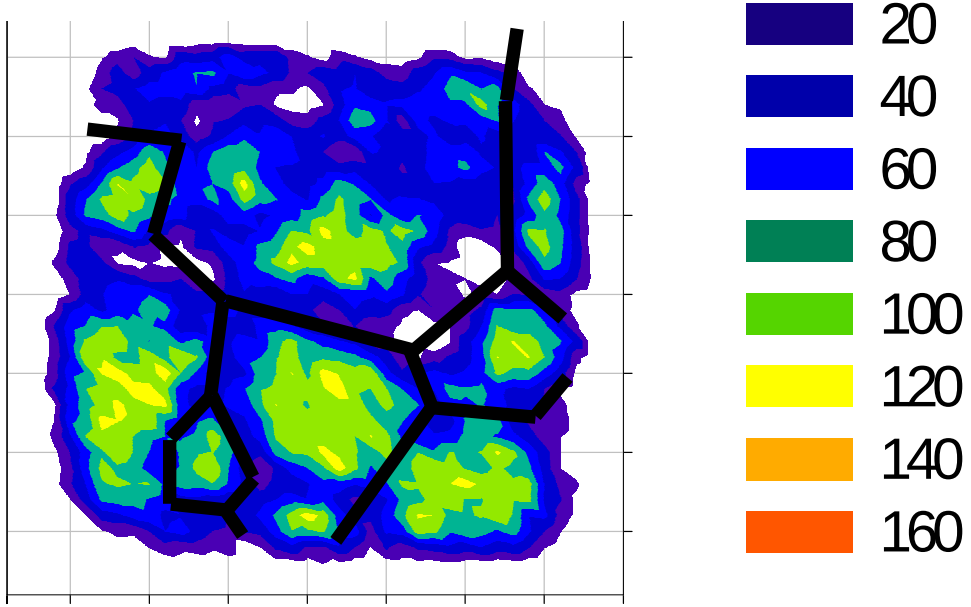

At 1000℃, depletion width > 3 μm

Helium diffusion higher near grain boundaries

Thermal diffusion of helium in uranium dioxide

Coupling various NRA techniques offers interesting possibilities to study helium in fuels

- Generating data to be used in fuel behavior code
- Providing mechanisms to be modeled
- Giving helium release stages as a function of temperature
- Demonstrating strong effects of microstructure , grain boundaries, to be taken into account in the transport mechanisms

Separated effects studies : illustrations

	Objective	Studies
1	Understand and model fission gas diffusion/ precipitation/release in nuclear oxide fuels	XAS and TEM characterization of Xe bubbles in uranium dioxide
2	Understand and model He behavior in nuclear oxide fuels	Thermal diffusion of helium in uranium dioxide
3	Oxygen diffusion in relation to p-type doping in UO_2	Electrical conductivity and diffusion coefficient measurements in UO_2

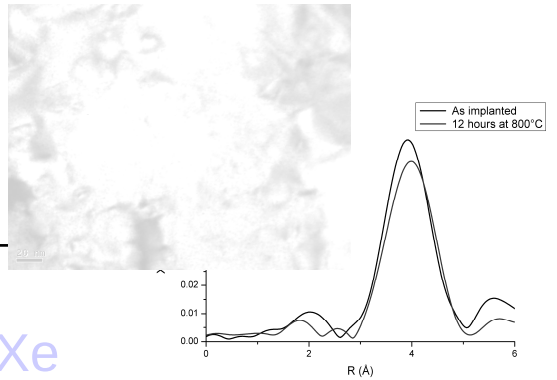

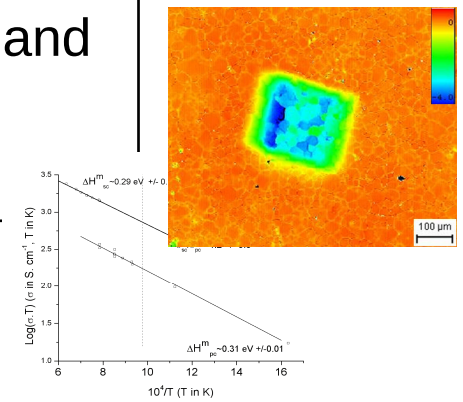

Oxygen diffusion in relation to p-type doping in UO_2

Aim: generate experimental data that can be compared to theoretical approaches, such as the nature of the defects, their migration mechanisms, …

Basic theory & Methodology

Combination of electrical conductivity and of intrinsic diffusion coefficients

Experimental

Techniques and materials

Electrical conductivity results

Diffusion coefficient measurements by secondary ion mass spectroscopy (**SIMS**)

Study led by Philippe Garcia (CEA-Cadarache)

P. Garcia, M. Fraczkiewicz, C. Davoisne, G. Carlot, B. Pasquet, G. Baldinozzi, D. Siméone, C. Petot, J. Nucl. Mater. (2010), in press.

Electrical conductivity of UO_2

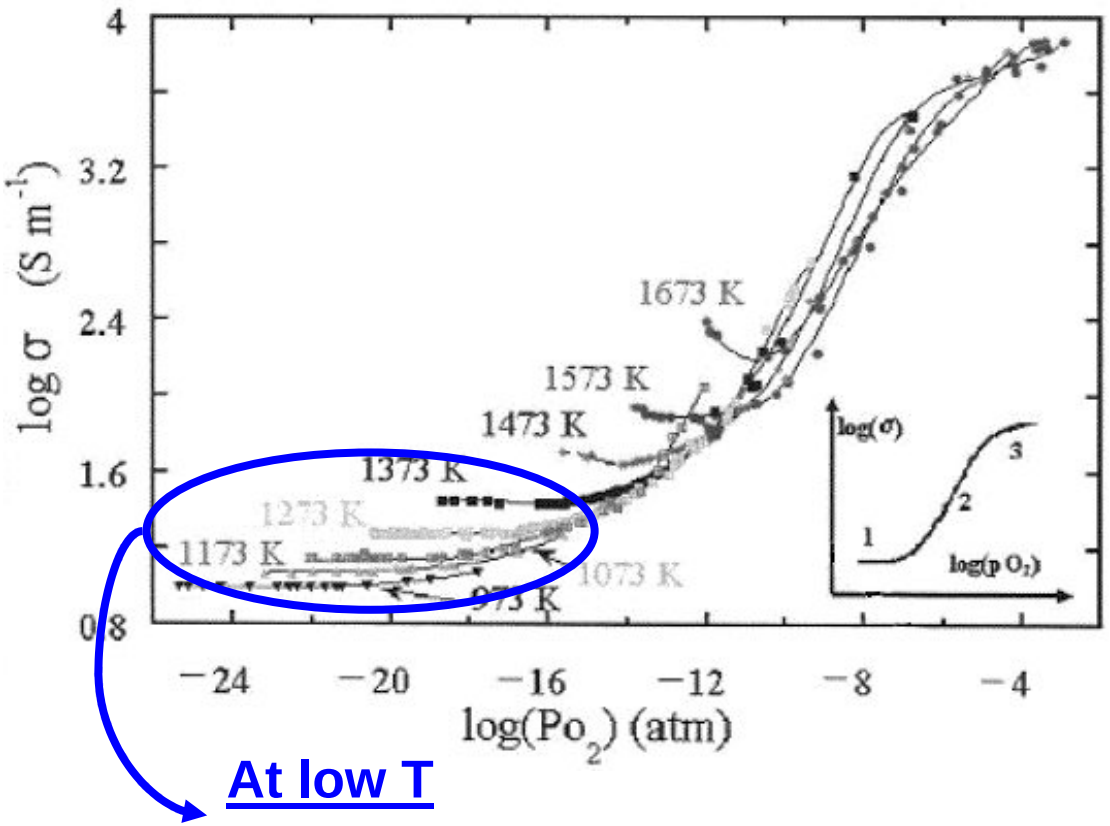

At low T

Low $p(O_2)$: extrinsic behaviour: charge carrier [h•] controlled by doping levels, σ independent of $p(O_2)$

At higher $p(O_2)$: intrinsic defects predominate, p-type charge carriers

At higher T:

n-type carriers at low $p(O_2)$

p-type charge carriers at high $p(O_2)$

P. Ruello *et al.* JACS 88, 604 (2005)

Basic equations, at low T, extrinsic regime

Expression for electrical conductivity yields the hole concentration **[h°]** and the enthalpy of migration **E^m**

$$\sigma = e.\mu^p.[h^\circ] = e.\frac{\mu_O^p.e^{\frac{-E_p^m}{k_b.T}}}{T}.[h^\circ]$$

"Simple" charged point defect model

$$\frac{1}{2}O_2 \rightleftharpoons O_i'' + 2.h^\circ \qquad \emptyset \rightleftharpoons O_i'' + V_O^{\circ\circ}$$

$$K_{O_i} = \frac{[O_i''].[h^\circ]^2}{\sqrt{p(O_2)}} \qquad K_{AF} = [O_i''].[V_O^{\circ\circ}]$$

Assumed equilibria

- **Interstitial mechanism** $D_O \propto [O_i''].e^{-\frac{E_m^{O_i}}{k_b T}}$
- **Vacancy mechanism** $D_O \propto [V_O^{\circ\circ}].e^{-\frac{E_m^{V_O}}{k_b T}}$

Objectives

Questions are:

- What mass balance equations?
  - Nature of defects assumed correct?
  - What diffusion mechanism for O?
  - Role of dopant concentration on diffusion properties ?
  - Migration energies, free energies for mass balance equations?

- **How do we check the theory?**
  - Take two materials containing **different doping levels**: single crystals (**SC**) / polycrystals (**PC**)
  - Measure σ : $\frac{\sigma_{sc}}{\sigma_{pc}} = \frac{[h^\circ]_{sc}}{[h^\circ]_{pc}} = r_\sigma$
  - Measure D_o: $\sqrt{\frac{D^O_{pc}}{D^O_{sc}}} \; ? \; \frac{1}{r_\sigma} \quad or \quad r_\sigma$

vacancy mechanism since

$$D_O \propto [V_O^{\circ\circ}].e^{-\frac{E_m^{V_O}}{k_b T}} \propto [h^\circ]^2$$

interstitial mechanism since

$$D_O \propto [O_i''].e^{-\frac{E_m^{O_i}}{k_b T}} \propto \frac{1}{[h^\circ]^2}$$

Materials used

- **Single crystals prepared from very large grain polycrystalline bloc**
  - Obtained from cooling of a molten mass of UO_2
  - **Grain size ~ 1-2mm**

element	P	SC
Cr	7	522
Fe	36	1649
Gd	9	
Mo	2	
Mn		59
Ca		1423
Ni		190
sum ppm	51	5516
Total concentration	1.2-2.1 $10^{18}cm^{-3}$	1.3-1.710$^{20}cm^{-3}$

- **Polycrystalline samples**
  - High density (98.5 % th.d) annealed at 1700℃ for 80 hours
  - **Grain size ~ 24 µm**

Electrical conductivity at low oxygen potential

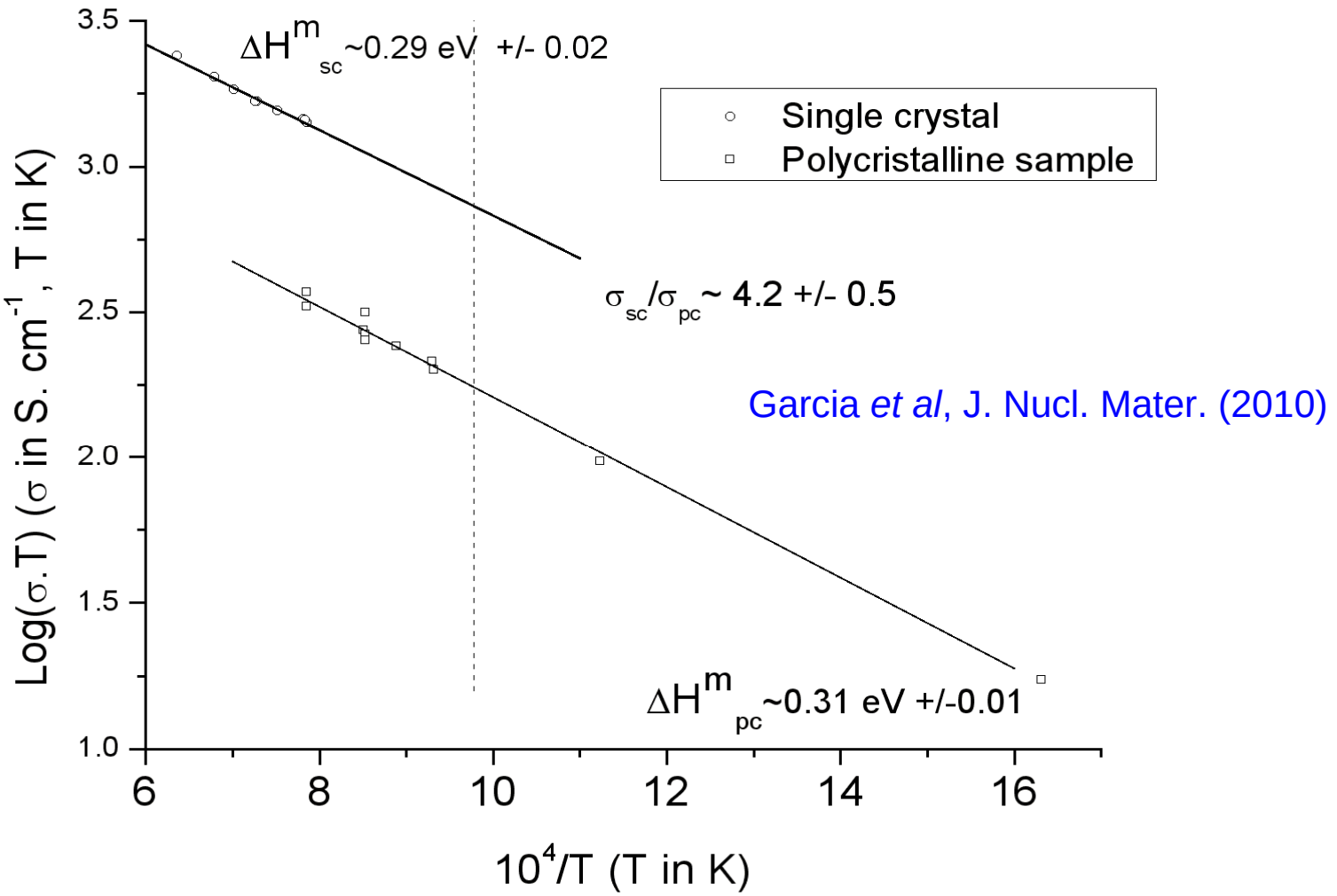

Garcia *et al*, J. Nucl. Mater. (2010)

Parallel lines: charge migration energy identical

Oxygen diffusion experiments in UO_2

- **Gas-solid isotopic exchange method**, vapour enriched in $^{18}O_2$
- **Annealing** conditions:
  - Simultaneous annealing of polycrystalline and single crystals
  - At 750℃ and lowest oxygen potential (~ 2.8 10^{-22} atm.)
- **SIMS** analysis of 2 samples
  - 10 kV Cs beam (beam current between 30-100 nA), 5 kV extraction field
  - beam rastered over 150x150 μm^2, extracted from an area 30 µm in diameter
  - Several craters in each sample
  - ^{16}O, ^{18}O, ^{235}U, $^{235}U^{16}O_2$ signals were systematically collected
- Crater depths determined using optical method (chromatic confocal microscopy)

Principles of SIMS

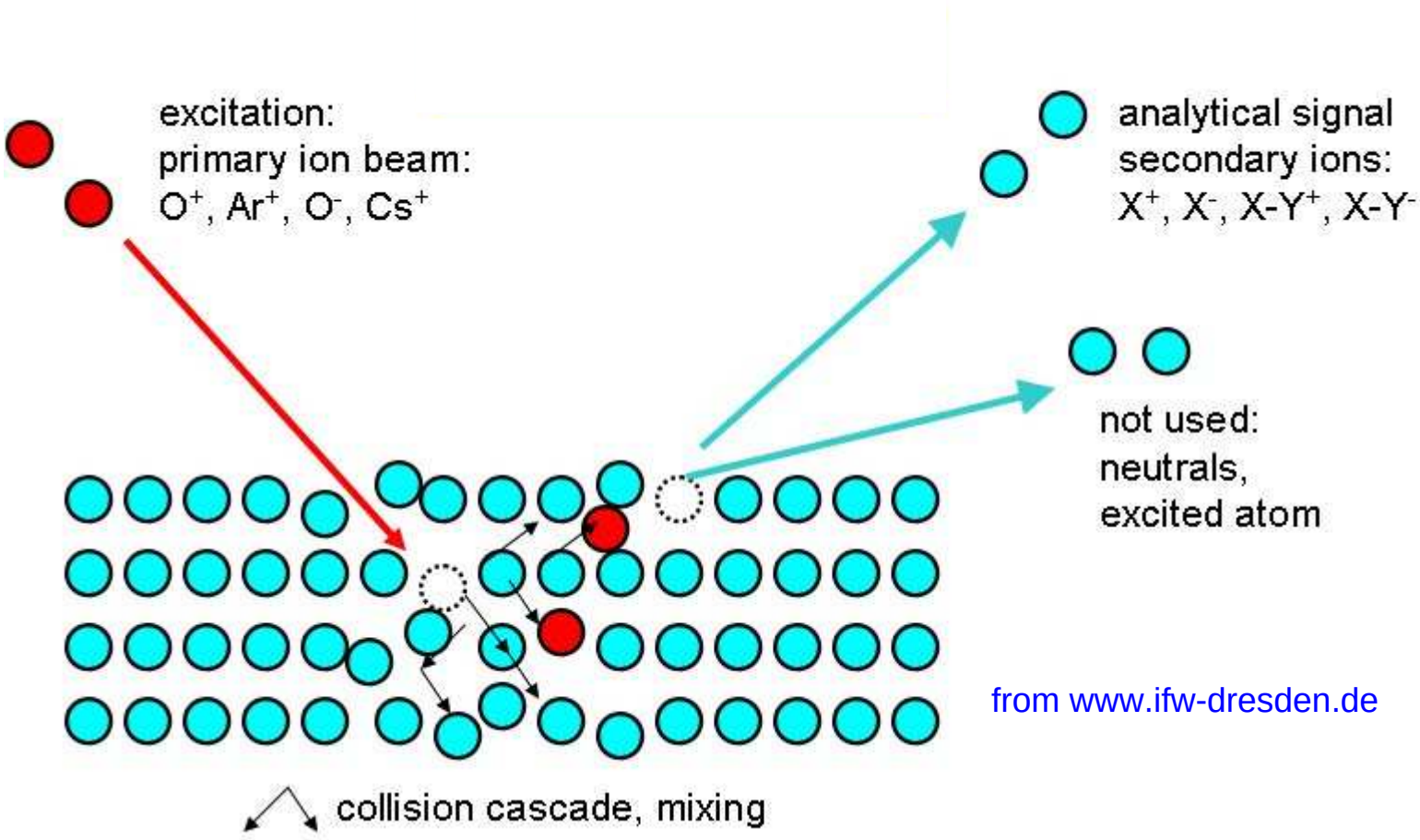

from www.ifw-dresden.de

Conversion time dependence to depth dependence yields chemical composition as a function of depth

Results obtained on a polycrystalline sample

$$\frac{\partial C_{^{18}O}}{\partial t} = \frac{\partial}{\partial z}\left(D\frac{\partial C_{^{18}O}}{\partial z}\right)$$

$$D.\frac{\partial C_{^{18}O}}{\partial z}_{surf.} = -k(C_g - C_{surf})$$

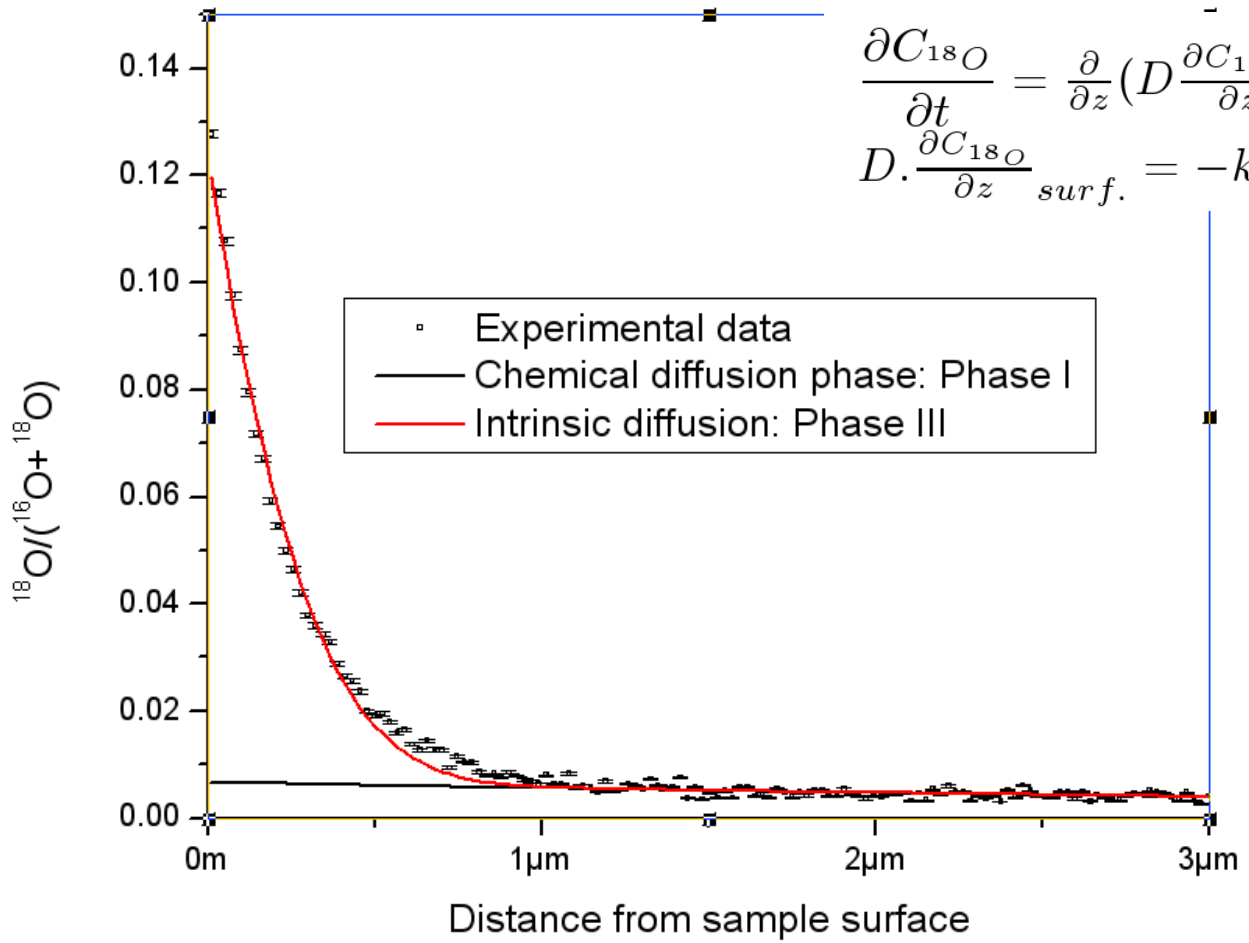

Model reproduces satisfactorily the experimental data

Garcia *et al*, J. Nucl. Mater. (2010)

Summary of the measurements

profile	$D(m^2.s^{-1})$	$k\ (m.s^{-1})$
S1	$5.4 \times 10^{-19} \pm 10^{-19}$	$4.8 \times 10^{-13}\ m^2.s^{-1} \pm 6 \times 10^{-14}$
S2	$6.4 \times 10^{-19} \pm 1.6 \times 10^{-19}$	$3.2 \times 10^{-13}\ m^2.s^{-1} \pm 4 \times 10^{-14}$
S3	$7.6 \times 10^{-19} \pm 10^{-19}$	$7.6 \times 10^{-13}\ m^2.s^{-1} \pm 8 \times 10^{-14}$
P1	$1.0 \times 10^{-17} \pm 3 \times 10^{-18}$	$4.5 \times 10^{-12}\ m^2.s^{-1} \pm 7 \times 10^{-13}$
P2	$1.4 \times 10^{-17} \pm 3 \times 10^{-18}$	$5.3 \times 10^{-12}\ m^2.s^{-1} \pm 6 \times 10^{-13}$
P3	$1.8 \times 10^{-17} \pm 2 \times 10^{-18}$	$5.7 \times 10^{-12}\ m^2.s^{-1} \pm 4 \times 10^{-13}$

Accurate determination of parameters

- $r = \sqrt{\frac{D_O^{pc}}{D_O^{sc}}}$ ~ 4.7 +/- 0.6 compared to 4.2 +/- 0.5 for $\left(\frac{\sigma_{sc}}{\sigma_{pc}}\right)$

$$D_O \propto \frac{1}{[h^\circ]^2}.\sqrt{p(O_2)}.K_{O_i}.e^{-\frac{\Delta H_m^{O_i}}{kT}} + [h^\circ]^2.\frac{K_{AF}}{K_{O_i}}.\frac{1}{\sqrt{p(O_2)}}.e^{-\frac{\Delta H_m^{V_O}}{kT}}$$

Concluding remarks and prospects

Efficient way of characterising nature of point defects and associated mass balance equations

- Relevant mass balance equation for UO_2:

$$\frac{1}{2}O_2 \rightleftharpoons O_i'' + 2.h^\circ$$

$$K_{O_i} = \frac{[O_i''].[h^\circ]^2}{\sqrt{p(O_2)}}$$

- In the extrinsic region studied, **doubly charged oxygen** interstitials are no doubt the point defects responsible for atomic migration

  First-principles calculations tell us it is an interstitialcy mechanism

- Oxygen defect concentrations are controlled at low T and $p(O_2)$ by impurity concentration on cation sublattice

- Prospects
  - Determine D_0 dependence on all parameters: oxygen potential, impurity concentration and temperature
  - Assess data against *ab initio* calculations
    - formation and migration energies
    - vibrational properties along migration paths

Part 4 conclusion

Necessary coupling between separated effects studies, PIE and fuel modeling

- **The separate effect studies** are complementary to the post irradiation examinations

- **The separate effect studies** enable us
  - to decorrelate and improve understanding of the relevant phenomena (thermal, irradiation, chemical effects)
  - Identification of mechanisms at lower scale
  - Determination of basic data to be used in the fuel behavior codes

→ **Essential to in-pile fuel behavior modeling**

→ **Essential to validate approximations in modeling**

General conclusion

- **Numerical and experimental simulations at the atomic scale of the fuel behavior under irradiation provide data, mechanisms to be used in fuel performance codes**

- **Various communities have to work together:**

- **modelling and experiment**
- **applied physics and basic research**

Acknowledgements

CEA Cadarache / Fuel Study Department
From the lab: C. Valot (head), M. Bertolus, B. Dorado, G. Martin, P. Garcia, P. Martin, G. Carlot, C. Sabathier, J. Durinck, C. Davoisne, M. Fraczkiewicz, H. Palancher, C. Martial, J.C. Dumas, J.P. Piron,
From the department : B. Pasquet, B. Michel, A. Bouloré, L. Noirot, P. Obry, Y. Guerin

CEA Saclay H. Khodja, C. Rapsaet, L. Van Brutzel, A. Chartier, JP. Crocombette, C. Gueneau
CEA Saclay – Ecole Centrale – CNRS : G. Baldinozzi, D. Siméone, C. Petot
CEA DAM F. Jollet, B. Amadon, G. Jomard, M. Torrent, F. Bottin
IRSN: R. Ducher

Imperial College (UK): R. Grimes, D. Parfitt
CNRS (F): MF. Barthe, T. Sauvage, P. Desgardin, E. Gilabert, F. Garrido
ITU (D): R. Konings, J. Somers, E. Kotomin, D. Gryaznov, P. van Uffelen, T. Wiss
SCK-CEN (B): K. Govers
NRG (NL): S. De Groot
ESRF FAME BL (F): O. Proux, J.-L. Hazemann, V. Nassif
TUM (D): N. Wieschalla, W. Petry, R. Jungwirth
AREVA-CERCA (F): C. Jarousse

ACTINET network of excellence

F-BRIDGE European project